# Predictions for off-shell $t\bar{t}Z$ production at the LHC: The complete set of LO and NLO contributions

**Daniele Lombardi**

Universität Würzburg, Institut für Theoretische Physik
und Astrophysik, 97074 Würzburg, Germany

daniele.lombardi@uni-wuerzburg.de

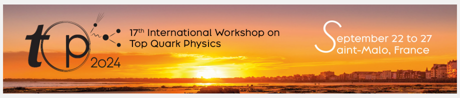


*The 17th International Workshop on*
*Top Quark Physics (TOP2024)*
*Saint-Malo, France, 22-27 September 2024*
doi:10.21468/SciPostPhysProc.18

## Abstract

**We present predictions for the production and decay of a top–antitop pair in association with a Z boson in the multi-lepton decay channel at the LHC. Our results include the complete set of LO and NLO contributions. Since our calculation is based on full matrix elements, off-shell effects are entirely taken into account. Integrated and differential cross-sections are reported for a realistic fiducial setup.**



Received 2024-10-21
Accepted 2024-12-18
Published 2026-01-29
doi:10.21468/SciPostPhysProc.18.014

## 1 Introduction

The relevance of the top-quark-associated Z-boson production ($t\bar{t}Z$ in the following) is nowadays well established and confirmed by the numerous searches that have been performed by experimental collaborations in the course of the Large Hadron Collider (LHC) life time. Indeed, its indepth investigation can offer for instance additional tests on the Standard Model (SM), better control on the background to other processes, and a direct access to the top-quark couplings with the electroweak (EW) sector.

For all these reasons, the theory community has tried hard in the last few decades to continuously improve the accuracy of the predictions for $t\bar{t}Z$ production. This problem has been tackled for a long time with simplified approaches, where typically resonance particles are set on shell or modelled with the narrow-width approximation. Only quite recently an off-shell calculation for $t\bar{t}Z$ in the four-charged-lepton decay channel came out in Ref. [1], where it was shown how crucial a correct modelling of the off-shell effects can be, especially for some differential observables. In that work, NLO accuracy in QCD was achieved. In this contribution, we discuss some results from Ref. [2], where all still-missing LO and NLO terms have been obtained with a full off-shell calculation. The same results were already presented in Ref. [3].

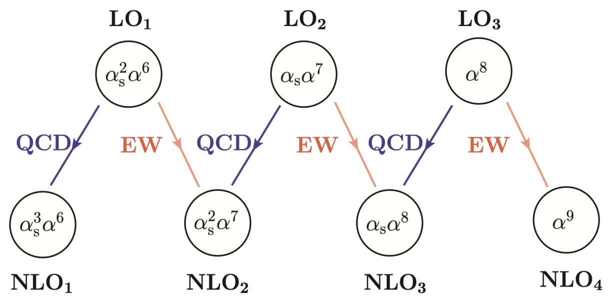


Figure 1: Perturbative orders contributing at LO and NLO for the process in Eq. (1).

## 2 Outline of the calculation

In Ref. [2] the different LO contributions and their NLO EW and QCD corrections to the process

$$\mathrm{pp} \to \mathrm{e}^+ \nu_\mathrm{e} \mu^- \overline{\nu}_\mu \mathrm{b}\,\overline{\mathrm{b}}\,\tau^+ \tau^- , \tag{1}$$

have been computed using the private Monte Carlo generator MoCaNLO. The latter program proved to be particularly efficient in dealing with processes with an intricate resonance structure, thanks to its highly-optimised multichannel integration. The code is interfaced with Recola [4, 5] and Collier [6], which allow for the numerical evaluation of all necessary tree-level SM matrix elements and one-loop integrals. A realistic modelling of off-shell effects is achieved by including the complete set of resonant and non-resonant Feynman diagrams. All relevant partonic channels have been considered, together with the photon- and bottom-induced ones. That has been done systematically for each of the perturbative orders contributing to the process (which are schematically summarized in Fig. 1).

## 3 Results

Our results have been obtained at a centre-of-mass energy of 13 TeV in the fiducial region described in Ref. [2]. Most notably, the infrared safety of the calculation when three bottom quarks occur in the final state has been ensured by proper recombination rules as part of the jet-clustering algorithm, where a b jet and a light jet are recombined into a b jet, and two b jets into a light jet. The factorization and renormalizaton scales have been set to $\mu_0 = \frac{1}{2}\left(M_{\mathrm{T,t}}\, M_{\mathrm{T,\bar{t}}}\right)^{1/2}$, which is based on the transverse masses of the reconstructed top/anti-top quarks. Theory uncertainties have been estimated with the standard 7-point scale variation.

### 3.1 Integrated cross-sections

Table 1 reports results for the integrated cross-sections at different perturbative accuracies, both without and including the bottom-channel contribution in $\sigma_{\mathrm{nob}}$ and $\sigma$, respectively. One can see that QCD corrections of NLO$_1$ type are the dominant ones, with a −10% K-factor and causing a large reduction in the size of the LO$_1$ uncertainty bands. The additional LO and NLO subleading contributions, which mostly cancel against each other, just correct the LO$_1$ result at the sub-percent level. We also observe that the inclusion of bottom-induced channels has a moderate impact of +1% on the full NLO prediction.

Table 1: LO cross-sections and NLO corrections (in ab) in the fiducial setup. In the second column all partonic channels are included in $\sigma_{\rm nob}$ except the ones having at least one bottom quark in the initial state, while $\sigma_{\rm b}$ includes all these channels. The sum of the two ($\sigma$) is shown in the sixth column. Ratios with respect to the cross-section $\sigma_{\rm nob}$ at $\rm LO_1$ accuracy are reported in the third and fifth column. In the seventh column ratios are shown with respect to the full $\rm LO_1$ cross-section including the bottom channels, as well. Integration errors are given in parentheses and percentage 7-point scale variations as super- and sub-scripts. See Ref. [3].

| perturbative order | $\sigma_{\rm nob}$ [ab] | $\frac{\sigma_{\rm nob}}{\sigma_{\rm nob,LO_1}}$ | $\sigma_{\rm b}$ [ab] | $\frac{\sigma_{\rm b}}{\sigma_{\rm nob,LO_1}}$ | $\sigma$ [ab] | $\frac{\sigma}{\sigma_{\rm LO_1}}$ |
|---|---|---|---|---|---|---|
| $\rm LO_1$ | $107.246(5)^{+35.0\%}_{-24.0\%}$ | 1.0000 | 0.31378(9) | +0.0029 | $107.560(5)^{+34.9\%}_{-23.9\%}$ | 1.0000 |
| $\rm LO_2$ | $0.7522(2)^{+11.1\%}_{-9.0\%}$ | +0.0070 | −0.6305(2) | −0.0059 | 0.1217(3) | +0.0011 |
| $\rm LO_3$ | $0.2862(1)^{+3.4\%}_{-3.4\%}$ | +0.0027 | 0.7879(2) | +0.0073 | $1.0742(3)^{+12.1\%}_{-14.9\%}$ | +0.0100 |
| $\rm NLO_1$ | −11.4(1) | −0.1072 | 0.518(3) | +0.0048 | −10.9(1) | −0.1016 |
| $\rm NLO_2$ | −0.89(1) | −0.0083 | 0.109(3) | +0.0010 | −0.78(1) | −0.0072 |
| $\rm NLO_3$ | 1.126(4) | +0.0105 | −0.089(4) | −0.0008 | 1.037(6) | +0.0096 |
| $\rm NLO_4$ | −0.0340(9) | −0.0003 | −0.0180(9) | −0.0002 | −0.052(1) | −0.0005 |
| $\rm LO_1+NLO_1$ | $95.8(1)^{+0.4\%}_{-11.2\%}$ | +0.8933 | 0.832(3) | +0.0078 | $96.6(1)^{+0.4\%}_{-10.7\%}$ | +0.8984 |
| LO | $108.285(5)^{+34.7\%}_{-23.8\%}$ | +1.0097 | 0.4713(3) | +0.0044 | $108.756(5)^{+34.5\%}_{-23.7\%}$ | +1.0111 |
| LO+NLO | $97.0(1)^{+0.5\%}_{-11.2\%}$ | +0.9052 | 0.991(6) | +0.0092 | $98.0(1)^{+0.4\%}_{-10.6\%}$ | +0.9114 |

### 3.2 Differential cross-sections

Fig. 2 shows the interplay of the different perturbative contributions for two illustrative observables. The distribution in transverse momentum of the $\rm b\bar{b}$ pair in Fig. 2a is extremely sensitivity in its tails to QCD corrections (in red), that manifest as a giant QCD K-factor. Nevertheless, subleading contributions provide important corrections to the observable in the same phase-space region: the $\rm NLO_2$ term (in green) can reach up to −15% of the $\rm LO_1$ at $p_{\rm T,b\bar{b}} = 700\,\rm GeV$, due to large EW Sudakov logarithms, and the $\rm NLO_3$ term (in goldenrod) a positive +5%. Even if the definition of this observable requires two b jets, the inclusion of bottom-induced channels just corresponds to a small normalisation effect over the full spectrum. Also for the invariant mass of the $\tau^+\tau^-$ pair in Fig. 2b accounting for perturbative orders beyond $\rm LO_1$ and $\rm NLO_1$ becomes crucial. The $\rm NLO_1$ dominates in the far off-shell region with a −20% correction to the $\rm LO_1$. In the same region, due to the growth of the photon PDF, photon contributions (in violet) turn out to be the most important subleading terms, with a K-factor up to +6%. Finally, the photon radiative effects included in the $\rm NLO_2$ term are the most significant ones right below the Z-boson resonance peak, where they amount to a +40% correction.

## 4 Conclusion

We have presented results for $\rm t\bar{t}Z$ production for 13 TeV proton–proton collisions that include the complete set of LO and NLO contributions and fully account for off-shell effects. Even if the impact of subleading corrections is moderate at the integrated level, they can cause significant shape distorsions for many observables. That renders their inclusion at the differential level crucial in view of precise phenomenology and a realistic description of the process.

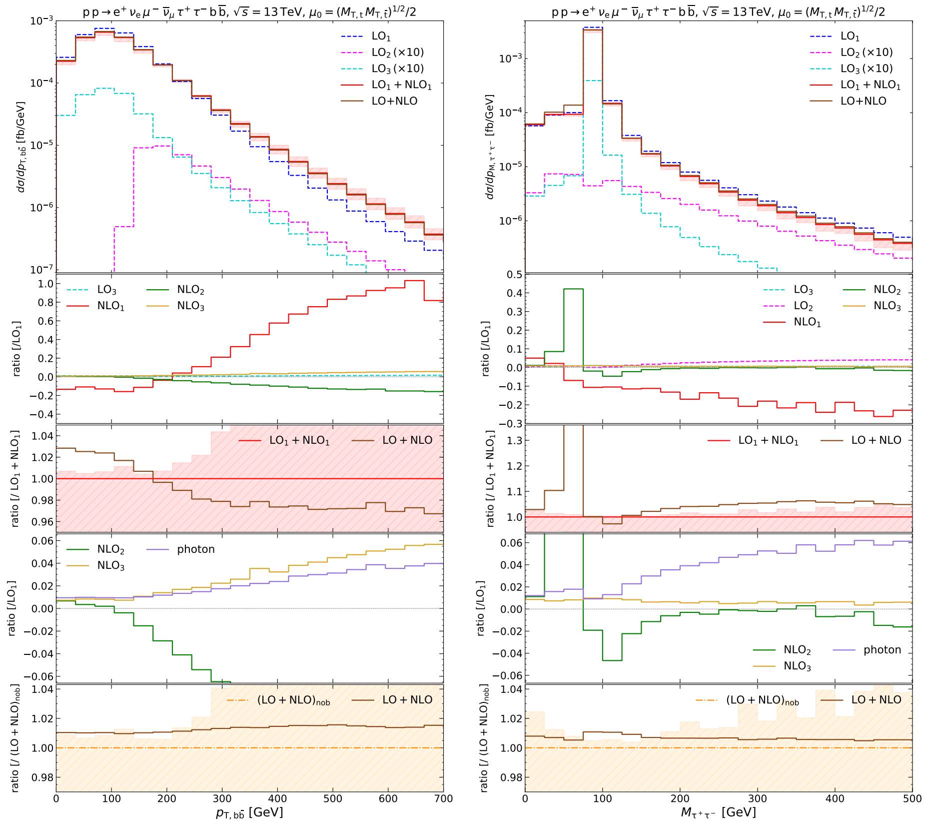


(a) Transverse momentum of the bottom-jet pair. (b) Invariant mass of the $\tau^+\tau^-$ pair.

Figure 2: Distributions in the transverse momentum of the bottom-jet pair (left) and in the invariant mass of the $\tau^+\tau^-$ pair (right). The different NLO corrections for the observables are compared separately (first ratio panels) and at the level of the full prediction (second ratio panel). The size of photon-induced channels and bottom contributions are presented in the third and fourth ratio panels, respectively. See Ref. [3].

## Acknowledgments

**Funding information** This contribution is based upon work supported by the German Federal Ministry for Education and Research (BMBF) under contract no. 05H21WWCAA.

## References

[1] G. Bevilacqua, H. Bayu Hartanto, M. Kraus, J. Nasufi and M. Worek, *NLO QCD corrections to full off-shell production of $t\bar{t}Z$ including leptonic decays*, J. High Energy Phys. **08**, 060 (2022), doi:10.1007/JHEP08(2022)060.

[2] A. Denner, D. Lombardi and G. Pelliccioli, *Complete NLO corrections to off-shell $t\bar{t}Z$ production at the LHC*, J. High Energy Phys. **09**, 072 (2023), doi:10.1007/JHEP09(2023)072.

[3] D. Lombardi, *Complete NLO corrections to off-shell $t\bar{t}Z$ production at the LHC*, Proc. Sci. **449**, 292 (2024), doi:10.22323/1.449.0292.

[4] S. Actis, A. Denner, L. Hofer, A. Scharf and S. Uccirati, *Recursive generation of one-loop amplitudes in the Standard Model*, J. High Energy Phys. **04**, 037 (2013), doi:10.1007/JHEP04(2013)037.

[5] S. Actis, A. Denner, L. Hofer, J.-N. Lang, A. Scharf and S. Uccirati, *RECOLA — REcursive Computation of One-Loop Amplitudes*, Comput. Phys. Commun. **214**, 140 (2017), doi:10.1016/j.cpc.2017.01.004.

[6] A. Denner, S. Dittmaier and L. Hofer, *Collier: A fortran-based complex one-loop library in extended regularizations*, Comput. Phys. Commun. **212**, 220 (2017), doi:10.1016/j.cpc.2016.10.013.